Passive and Active Deformation Processes of 3D Fibre-Reinforced Caricatures of Cardiovascular Tissues

Antonio DiCarlo[1], Paola Nardinocchi[2], Tomás Svatoň[3], and Luciano Teresi[*,1]
[1]Modeling & Simulation Lab, University "Roma Tre", Italy;
[2]Dept. Structural Engineering & Geotechnics, University of Rome "La Sapienza", Italy;
[3]Dept. Mathematics, University of West Bohemia, Czech Republic.
[*]Corresponding author: Via C. Segre 2, 0146 Roma, Italy; teresi@uniroma3.it

Abstract: In this paper, we present a mathematical model of contractile elastic solids meant to simulate various districts of the cardiovascular system, and based on the concepts of active deformation and embedded muscle fibres.

Specifically, here we deal with the modelling of the gross mechanics of the left ventricle (LV) which is strictly related to its pump function. The muscle fibres embedded in the LV walls govern, through their contraction and relaxation, the characteristic phases of the cardiac cycle. Moreover, muscle fibres define the anisotropy directions of the LV wall, and the collagene fibres determine the material properties along these directions; thus, to model the mechanical behaviour of the LV, both the passive and the active material properties of the must be accurately accounted for. As is well known, the effectiveness of the pumping action is well represented by the pressure-volume (PV) diagrams that relate the blood pressure to the volume of the LV during the cardiac cycle. Here, we aim at reproducing realistic PV by specifying appropriate sequence of muscle contraction

Keywords: Biomechanics, muscle modelling, fibre-reinforcedd materials, active contractions.

1 Introduction

A key issue in the modelling of biological tissues is the active nature of muscle fibres, in other words, their ability to contract and relax in response to biochemical signals. Such a behaviour is commonly accounted for through an additive decomposition of the stress into a standard component, representing the passive response of the tissue, typically (visco-)elastic, and a nonstandard active component, meant to represent the dynamical effects of muscle contraction [1].

We favour a different modelling perspective, in which muscle contraction is accounted for by introducing the notion of *active deformation*: we assume that the contraction experienced by a muscle fibre under stimulus is described at the macroscopic scale by a (stress-free) change in the length of the fibre; the visible length of the fibre, in turn, depends on the amount of stress it sustains. To avoid a key misleading, it is worth saying that the notion of "active state"–a physiologic notion for muscles, coincides with that of "ground state"–a mechanical notion for elastic bodies. Thus, the active deformation describes how a muscular tissue shortens once activated and left free to contract, while the visible deformation describes the state that a muscular tissue attains once contracted, loaded and/or kinematically constrained (as in isometric activation).

The corresponding material model is based on a two-layer kinematics, comprising the classical vector-valued displacement field, plus a tensor-valued field parameterizing the evolving stress-free state of muscular tissue. This viewpoint, anticipated by the linearized 1D model introduced in [2], was developed in [3], [4], and [5] into a full-fledged nonlinear 3D theory, along the lines set forth by the theory of material remodelling [6], [7].

2 Muscle Modeling

Let the body $\mathcal{B}$ be a smooth region (with boundary $\partial\mathcal{B}$) of the three dimensional Euclidean space $\mathcal{E}$, and $\mathcal{V}$ the linear space of translations associated to $\mathcal{E}$; a displacement of $\mathcal{B}$ is described by a smooth vector field

$$\mathbf{u}: \quad \mathcal{B} \to \mathcal{V}; \tag{2.1}$$

thus, $x = X + \mathbf{u}(X)$ denotes the position of a material point $X \in \mathcal{B}$. The *visible* deforma-

tion of the body is described by the gradient $\mathbf{F} = \mathbf{I} + \nabla\mathbf{u}$ of the displacement, where is $\mathbf{I}$ the identity tensor.

2.1 Fibres architecture

The architecture of the muscle fibres dictates the activation line of the tissue, that is, the direction along which muscular fibres contract. This microstructurally relevant direction is determined by the fibre axis, described by specifying a unit-vector field $\mathbf{f}_o$ on $\mathcal{B}$.

Here, we shall consider a conceptual geometry, a cylindrical pipe , representing a coarse model of a heart ventricle; moreover, we represent muscle fibres as helicoidal fibres. Given an orthonormal frame $\{o; \mathbf{e}_1, \mathbf{e}_2, \mathbf{e}_3\}$ for $\mathcal{E}$, and a system of Cartesian coordinates $X = o + x\,\mathbf{e}_1 + y\,\mathbf{e}_2 + z\,\mathbf{e}_3$, we define a polar system of coordinates

$$(r, \theta, z) \mapsto X = o + r\,\mathbf{n}(\theta) + z\,\mathbf{e}_3\,, \qquad (2.2)$$

with $\mathbf{n}(\theta) = \cos\theta\,\mathbf{e}_1 + \sin\theta\,\mathbf{e}_2$, $0 < \theta < 2\pi$. Given a pipe with axis $\mathbf{e}_3$, a helicoidal fibre of pitch b is described by a curve whose unit tangent vector $\mathbf{f}_o$ is given by

$$\mathbf{f}_o = \frac{r}{(r^2 + b^2)^{\frac{1}{2}}}\,\mathbf{n}_{,\theta} + \frac{b}{(r^2 + b^2)^{\frac{1}{2}}}\,\mathbf{e}_3\,, \qquad (2.3)$$

with $\mathbf{n}_{,\theta} = \partial\mathbf{n}/\partial\theta$; for $b = 0, \infty$ equation (2.3) defines circumferential or axial fibres, respectively.

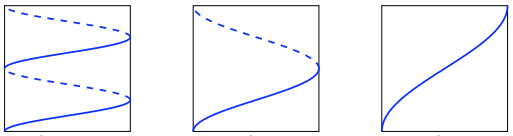

Figure 1: Helical fibres with different pitches, winding along a cylindrical body of height h.

2.2 Active Response

We assume as primary the notion of contraction: it is measured macroscopically by the variation in the rest length of the muscle fibre through the distortion field $\mathbf{F}_o : \mathcal{B} \to \mathbb{L}\mathtt{in}$ to be known as the *active deformation* field. The muscle fibre architecture enters the model by assigning a specific structure to the active deformation field:

$$\mathbf{F}_o = \delta\,\mathbf{f}_o \otimes \mathbf{f}_o + \check{\mathbf{I}}\,, \quad \check{\mathbf{I}} = \mathbf{I} - \mathbf{f}_o \otimes \mathbf{f}_o\,, \qquad (2.4)$$

with $\mathbf{I}$ the identity tensor. Let us note that the choice of a specific representation for the active deformation tensor $\mathbf{F}_o$ is an important constitutive issue; here, in the absence of any strong physiological arguments dictating a particular choice, we select a uniaxial tensor sharing one eigenvector with the fibre director $\mathbf{f}_o$. Thus, $\mathbf{F}_o\,\mathbf{f}_o$ is a ground state for the fibre $\mathbf{f}_o$, and the component

$$\delta = \mathbf{F}_o\,\mathbf{f}_o \cdot \mathbf{f}_o \qquad (2.5)$$

of the active deformation along the fibre axis measures the contraction of that fibre. Within our theory, the parameter δ is a link between mechanics and electrophysiology: action potential and calcium release regulate the time course of contraction. A coupled model based on the notion of active contractions, and accounting for electromechanical effects has been presented in [4] , [5].

The *elastic deformation* $\mathbf{F}_e$ of a fibre measures the difference between its active state $\mathbf{F}_o\,\mathbf{f}_o$, and the visible one $\mathbf{F}\,\mathbf{f}_o$: it is defined in the sense of the multiplicative composition by[1]

$$\mathbf{F}_e = \mathbf{F}\,\mathbf{F}_o^{-1}\,. \qquad (2.6)$$

As usual, the elastic strain is measured through the left Cauchy-Green tensor $\mathbf{C}_e$ associated with $\mathbf{F}_e$:

$$\mathbf{C}_e = \mathbf{F}_e^{\top}\mathbf{F}_e = \mathbf{F}_o^{-\top}\mathbf{C}\,\mathbf{F}_o^{-1}\,, \quad \mathbf{C} = \mathbf{F}^{\top}\mathbf{F}\,. \qquad (2.7)$$

Let us note that $\mathbf{C}_e$ measures the strain λ_e suffered by a contracted fibre $\mathbf{f}$ once it has been embedded in the actual state, (see figure 2)

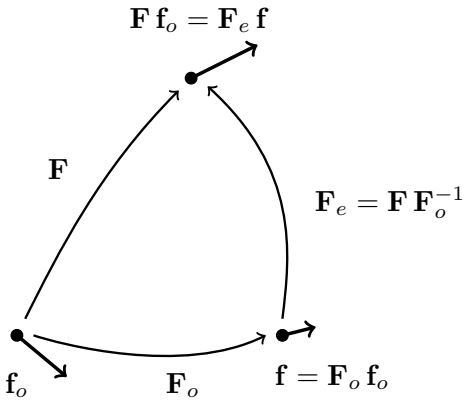

Figure 2: The material fibre $\mathbf{f}_o$ is mapped by the tensor field $\mathbf{F}_o$ to its contracted state $\mathbf{f}$; the elastic strain it suffers is measured by $\mathbf{F}_e$.

[1] It is worth noting that $\mathbf{F}_o$ and $\mathbf{F}_e$ are not, in general, gradients of any fields.

$$\lambda_e^2 = \mathbf{F}_e\,\mathbf{f}\cdot\mathbf{F}_e\,\mathbf{f} = \mathbf{C}_e\cdot\mathbf{f}\otimes\mathbf{f}\,. \tag{2.8}$$

2.3 Passive Response

Let us introduce the isochoric part $\bar{\mathbf{F}}_e$ of the elastic deformation $\mathbf{F}_e$

$$\bar{\mathbf{F}}_e = (J_e)^{-1/3}\,\mathbf{F}_e\,,\quad J_e = \det\mathbf{F}_e\,, \tag{2.9}$$

and define a strain $\bar{\mathbf{C}}_e$ measuring only isochoric deformations

$$\bar{\mathbf{C}}_e = \bar{\mathbf{F}}^{\top}{}_e\,\bar{\mathbf{F}}_e\,. \tag{2.10}$$

Here, we assume a passive material response described through a transversely isotropic strain-energy density (per unit of ground volume)

$$\psi : \mathbf{C}_e \mapsto \psi(\mathbf{C}_e) = \psi_s(\bar{\mathbf{C}}_e) + \psi_v(J_e)\,, \tag{2.11}$$

made of an isochoric contribution ψ_s, and a volumetric one ψ_v. Following [11], the isochoric term is further decomposed into an isotropic part ψ_{iso}, plus an anisotropic term ψ_f, accounting for the fibres reinforcement, and effective only for a positive fibres stretching, that is, for $\lambda_e > \delta$:

$$\psi_s(\bar{\mathbf{C}}_e) = \psi_{iso}(\bar{\mathbf{C}}_e) + f(\lambda_e)\,\psi_f(\bar{\mathbf{C}}_e)\,, \tag{2.12}$$

with

$$f(\lambda_e) = \begin{cases} 1, & \lambda_e > \delta\,; \\ 0, & \lambda_e \le \delta\,; \end{cases} \tag{2.13}$$

and

$$\begin{aligned} &\psi_{iso} = \tfrac{\mu}{2}\,(I_1(\bar{\mathbf{C}}_e) - 3)\,, \\ &\psi_f = \tfrac{\mu}{2}\,[\,(\gamma_4\,(I_4(\bar{\mathbf{C}}_e) - 1)^2 + \gamma_5\,(I_5(\bar{\mathbf{C}}_e) - 1)^2\,]\,. \end{aligned} \tag{2.14}$$

The three invariants I_i of $\bar{\mathbf{C}}_e$ are defined as

$$\begin{aligned} I_1(\bar{\mathbf{C}}_e) &= \bar{\mathbf{C}}_e\cdot\mathbf{I}\,, \\ I_4(\bar{\mathbf{C}}_e) &= \bar{\mathbf{C}}_e\cdot\mathbf{f}_o\otimes\mathbf{f}_o\,, \\ I_5(\bar{\mathbf{C}}_e) &= \bar{\mathbf{C}}_e^2\cdot\mathbf{f}_o\otimes\mathbf{f}_o\,. \end{aligned} \tag{2.15}$$

Finally, the volumetric component assumes the standard form

$$\psi_v(J_e) = \frac{1}{2}\,k(J_e - 1)^2\,, \tag{2.16}$$

with k the bulk modulus.

2.4 Stress Measures

The definition of a strain-energy density per unit ground volume (2.11) deserves some attention in the procedure delivering the constitutive stress measures [6], see diagram in figure 3: the energetic stress measure $\mathbf{S}_o$ (aka, Piola-Kirchhoff stress) is given by

$$\mathbf{S}_o = \frac{\partial\psi}{\partial\mathbf{F}_e} = 2\mathbf{F}_e\,\mathbf{S}_c\,,\quad \mathbf{S}_c = \frac{\partial\psi}{\partial\mathbf{C}_e}\,. \tag{2.17}$$

The reference stress $\mathbf{S}$ is the pull-back of $\mathbf{S}_o$ through the cofactor $\mathbf{F}_o^* := J_o\,\mathbf{F}_o^{-\top}$ of $\mathbf{F}_o$, where $J_o = \det\mathbf{F}_o$:

$$\mathbf{S} = \mathbf{S}_o\,\mathbf{F}_o^* = 2J_o\mathbf{F}\,(\mathbf{F}_o^{-1}\,\mathbf{S}_c\,\mathbf{F}_o^{-\top})\,. \tag{2.18}$$

Finally, the actual stress (aka, Cauchy stress) is the push-forward of $\mathbf{S}$ through $\mathbf{F}$,

$$\mathbf{T} = J^{-1}\mathbf{S}\mathbf{F}^{\top},\quad J = J_o\,J_e\,. \tag{2.19}$$

Let us note that as a consequence of the additive splitting of the energy, we have that the energetic stress $\mathbf{S}_c$ turns out to be the sum of three terms:

$$\mathbf{S}_c = \mathbf{S}_{c,iso} + f(\lambda_e)\,\mathbf{S}_{c,f} + \mathbf{S}_{c,v}\,. \tag{2.20}$$

with

$$\mathbf{S}_{c,iso} = \frac{\partial\psi_{iso}}{\partial\mathbf{C}_e}\,,\quad \mathbf{S}_{c,f} = \frac{\partial\psi_f}{\partial\mathbf{C}_e}\,,\quad \mathbf{S}_{c,v} = \frac{\partial\psi_v}{\partial\mathbf{C}_e}\,. \tag{2.21}$$

It follows that the stress $\mathbf{T}$ may be written as

$$\mathbf{T} = \mathbf{T}_s + k\,(J_e - 1)\,\mathbf{I} \tag{2.22}$$

with

$$\mathbf{T}_s = 2\,J^{-1}\,J_o\,\mathbf{F}_e\,(\mathbf{S}_{c,iso} + f(\lambda_e)\,\mathbf{S}_{c,f})\,\mathbf{F}_e^{\top}\,. \tag{2.23}$$

The spherical part of $\mathbf{T}$ identifies a constitutive prescription for the pressure:

$$p = -k\,(J_e - 1)\,, \tag{2.24}$$

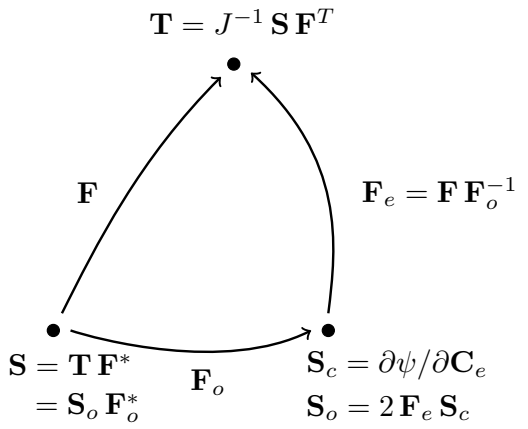

Figure 3: Stress measures and their relationships.

which allows to write, as usual, $\mathbf{T} = \mathbf{T}_s - p\,\mathbf{I}$. Accordingly, the reference stress $\mathbf{S}$ may be written as $\mathbf{S} = \mathbf{S}_s + \mathbf{S}_v$, with

$$\begin{aligned} \mathbf{S}_s &= 2\,J_o\,\mathbf{F}_e\,(\,\mathbf{S}_{c,iso} + f(\lambda_e)\,\mathbf{S}_{c,f}\,)\,\mathbf{F}_o^{-\top} \\ \mathbf{S}_v &= k\,(J_e - 1)\mathbf{F}^* = -p\,\mathbf{F}^*\,. \end{aligned} \tag{2.25}$$

2.5 Balance

The balance equations are formulated in integral form on the reference configuration $\mathcal{B}$: for any admissible test velocity $\widetilde{\mathbf{u}}$ it holds

$$\int_{\mathcal{B}} (-\mathbf{S}\cdot\nabla\tilde{\mathbf{u}} + \mathbf{f}\cdot\widetilde{\mathbf{u}}) + \int_{\partial\mathcal{B}} \mathbf{t}\cdot\tilde{\mathbf{u}} = 0\,, \tag{2.26}$$

with $\mathbf{f}$ the bulk force and $\mathbf{t}$ the traction field on $\partial\mathcal{B}$. Standard localization arguments yield the balance of forces in PDE form

$$\begin{aligned} &\operatorname{div}\mathbf{S} + \mathbf{f} = 0\,, \quad \text{on} \quad \mathcal{B}\,, \\ &\mathbf{S}\,\mathbf{m} = \mathbf{t}\,, \quad \text{on} \quad \partial\mathcal{B}\,, \end{aligned} \tag{2.27}$$

with $\mathbf{m}$ the outward normal to $\partial\mathcal{B}$.

3 Use of COMSOL Multiphysics

We implemented the whole problem from scratch in a COMSOL script: parametric geometry, balance equations in weak form (inclusive of boundary conditions), and constitutive prescriptions. We used this code to investigate the combined passive-active response of reinforced cylindrical pipes and ellipsoidal thick shells (dummies of the left ventricle), with varied fibre architectures.

We solve the balance equations (2.26) using a mixed displacement-pressure formulation: assuming null bulk force, the problem is to find a displacement field $\mathbf{u}$ and a pressure field p such that

$$\begin{aligned} &\int_{\mathcal{B}} -(\mathbf{S}_s - p\,\mathbf{F}^*)\cdot\nabla\tilde{\mathbf{u}} + \int_{\partial\mathcal{B}} \mathbf{t}\cdot\tilde{\mathbf{u}} = 0 \\ &\int_{\mathcal{B}} (\frac{p}{k} + (J_e - 1))\,\tilde{p} = 0\,, \end{aligned} \tag{3.28}$$

for all test field $\tilde{\mathbf{u}} \in \mathcal{L}^2_o$ and $\tilde{p} \in \mathcal{L}^1$, where $\mathcal{L}^i$ denotes the space of piecewise polynomials of degree i, and $\mathcal{L}^i_o$ its subspace compatible with the kinematics boundary conditions. For the inflation tests, the traction $\mathbf{t}$ represents the pull-back of a pressure field π acting on the inner mantle:

$$\mathbf{t} = -\pi\,\mathbf{F}^*\mathbf{m}\,; \tag{3.29}$$

moreover, the volume of the inner cavity $\mathcal{C}_t$ in the deformed configuration has been computed as a boundary integral on $\partial\mathcal{C}$ using the formula

$$\operatorname{Vol}(\mathcal{C}_t) = \frac{1}{3}\int_{\mathcal{C}_t} \operatorname{div}(x) = \frac{1}{3}\int_{\partial\mathcal{C}} (X+\mathbf{u})\cdot\mathbf{F}^*\,\mathbf{m}\,. \tag{3.30}$$

Step function (2.13) has been implemented using a smoothed Heaviside function.

4 Results

Specific aim of the work is to investigate the response of the left ventricle to assigned pressure cycles. The response depends on some global quantities such as the shape of the LV–like body and the muscle fibre architecture; our choices about these two elements have been discussed in section 2. Other key issues in the analysis of the LV response is due to the characterization of the passive and active material response of the cardiovascular tissue comprising the LV walls which has been presented in section 2, too.

Here, we discuss the influence of these elements on the mechanical performance of the left ventricle; specifically, we aim to stress the capacity of our distinguished notion of active deformation in capturing some essential mechanical features of myocardium contraction. Precisely, we specify appropriate pressure and contraction cycles and aim at reproducing realistic PV loops which are relevant elements characterising heart performances [8], [9].

4.1 Traction Test

As equations (2.11)-(2.16) show, the passive material response of the tissue is assumed to be (locally) transversely isotropic and non homogeneous (due to the variable pitch of the helices across the wall thickness). Actually, the cardiovascular tissue comprising the LV walls shows a relevant global anisotropic response which allows to distinguish circumferential and longitudinal directions. Hence, as first, we simulate traction tests on a model specimen whose passive response be described through the strain energy density (2.11)-(2.16) and tune the material parameters so to recover the anisotropic behaviour described in [12]. Specifically, we consider an affine variation of the angle shared by the muscle fibres and the horizontal plane through the wall, running from $60°$ (on the inner wall) to $-60°$ (on the outer wall). Then, we suppose to handle a model specimen extracted from the cylinder wall and perform two traction tests, along the longitudinal (vertical) and the circumferential direction (see figure 4). As figure (5) shows, a suitable tuning of the shear modulus μ and the stiffness parameters γ_4 and γ_5 makes it possible to capture the overall anisotropic characteristics of the material related to the passive material response of the myocardium along the circumferential and longitudinal directions.

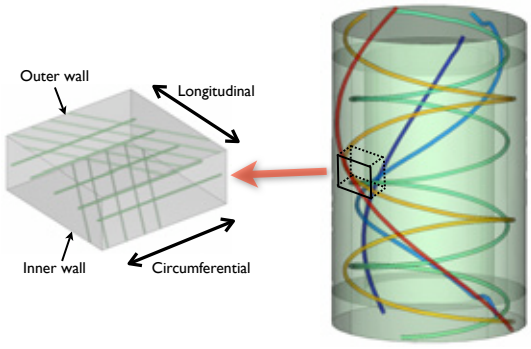

Figure 4: Traction test on the model specimen; the angle between fibres and horizontal plane runs form $-60°$ on the outer wall (epicardium) to $60°$ on the inner wall (endocardium).

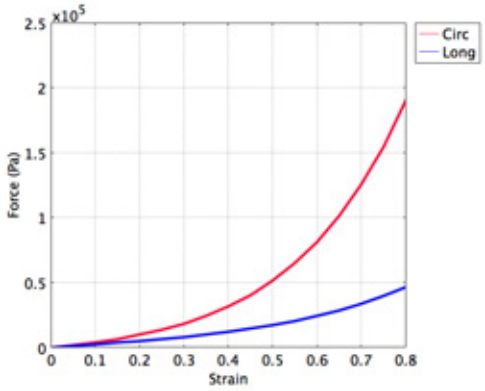

Figure 5: Traction test. The circumferential response is roughly three times stiffer than the longitudinal one.

4.2 Pressure–Volume loops

Here, we fix the passive material response of the myocardium completely defined by the equations (2.11)-(2.16) and by the material parameters listed in Table 1. As first, we reproduce a typical PV loop by solving a sequence of elastic problems whose input are pairs pressure-contraction. Pressure π ranges from 10 mmHg to 120 mmHg and contraction δ from 1 to about 0.7. There is a large difference between these two kind of data. Actually, the pressure cycle may be easily measured and it is well known how it changes in presence of heart diseases. On the contrary, the contractility of the wall tissue is far from being well defined. Usually, it is assumed that the so–called systolic elastance represents well enough the contractile capacity of the myocardium which in our model is measured by the field δ. Hence, the contraction cycles we assign here are not derived from measures performed on patients as the pressure cycles are. Actually, we tune the contraction cycle in such a way that a suitable PV loop may be performed by our cylindrical model.

The results we derive are promising. Figure (6) shows that within the context of our modeling it is possible to pick up the pressure–volume loop in an efficient way. Moreover, figure (8) shows the sensitivity of the model to change in the assumptions on the angles shared by the muscle fibres and the horizontal plane.

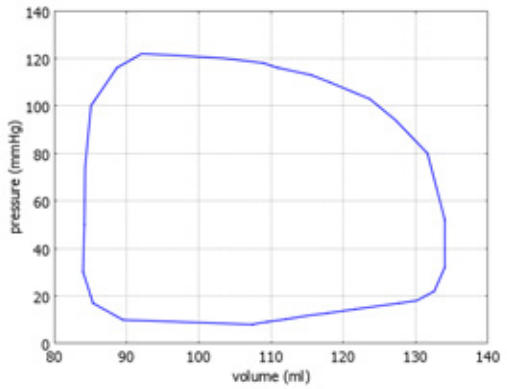

Figure 6: Pressure-Volume relationship for a pipe whose helically wound fibres have varying pitch: the angle between fibres and horizontal plane runs form -60° on the epicardium to 60° on the endocardium.

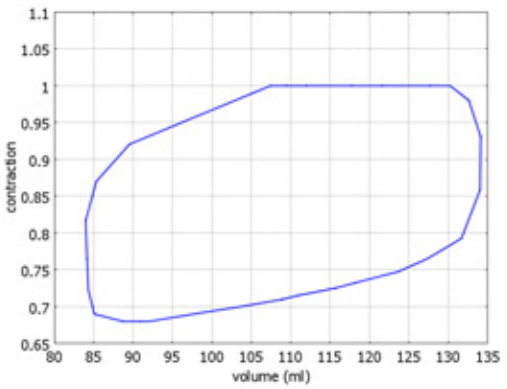

Figure 7: Contraction-Volume relationship for a pipe; helically wound fibres are as described in previous figure.

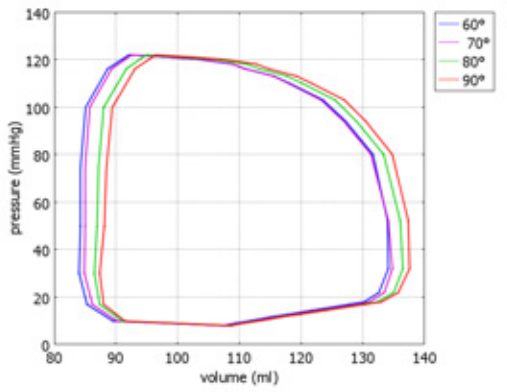

Figure 8: Sensitivity to fibres pitch of pressure-volume relationship for a helically wound pipe. Label shows the range of the angle between fibres and horizontal plane.

It is interesting to look at another typical loop which usually is discussed in literature with reference to the single muscle cell ([13]) (in such a case, contraction is intended to measure the shortening of the sarcomere): the contraction–volume loop. Figure 7 shows this kind of cycle when tissue contraction is measured through our notion of contractility (a macroscopic notion). Interestingly, the picture in figure (7) resembles the cycles shown in [13] where sarcomere shortening is represented versus left ventricular volume at any time along a typical cardiac cycle, see figure 9.

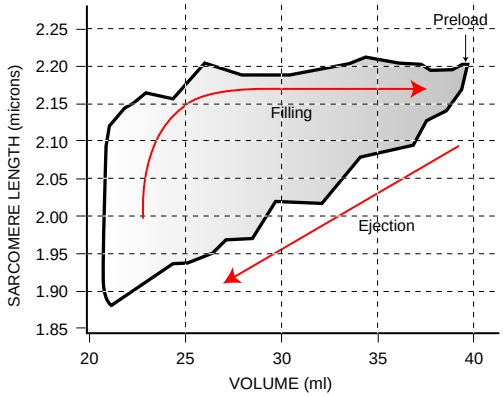

Figure 9: Reconstructed sarcomeres length during a cardiac cycle for a canine heart. Adapted from [13].

Parameter	Symbol & Value
Reference volume	92 ml
Shear modulus (pipe)	$\mu = 6e3$ Pa
Fibre stiffness	$\gamma_4 = 1.00$
Fibre stiffness	$\gamma_5 = 0.15$

Table 1: Numerical values of parameters.

5 Conclusion

The present work represents a proof of concept: we aimed at investigating the prospects of the use of the notion of active contraction, and its capability in capturing some essential mechanical features of myocardium contraction. Future directions are multifold: main themes are improving the geometry, especially the fibre architecture; adopting a fully anisotropic strain energy instead of the transversely anisotropic one; coupling the contraction parameter with an electro-physiological model apt to describe the spreading of action potential along the myocardial tissue.

References

[1] R. S. Chadwick. Mechanics of the Left Ventricle, Biophysical Journal, 39 (1982).

[2] P. Pelce, J. Sun. A simple model for excitation-contraction coupling in the heart. Chaos, Solitons & Fractals **5**, 383–391, (1995).

[3] P. Nardinocchi, L. Teresi. On the Active Response of Soft Living Tissues. J. Elasticity, 88, 27-39 (2007).

[4] C. Cherubini, S. Filippi, P. Nardinocchi, L. Teresi. An electromechanical model of cardiac tissue: Constitutive issues and electrophysiological effects. Progress in Biophysics and Molecular Biology, **97**, 562-573 (2008).

[5] C. Cherubini, S. Filippi, P. Nardinocchi, L. Teresi. Electromechanical models of cardiac tissues. In "Mechanosensitivity in Cells and Tissues: Mechanosensitivity of the Heart", eds. Kamkin & Kiseleva, "Springer" (2009).

[6] A. DiCarlo, S. Quiligotti. Growth and balance. Mechanics Research Communications **29** (2002).

[7] M. Tringelová, P. Nardinocchi, L. Teresi, A. DiCarlo. The cardiovascular system as a smart system. Topics on Mathematics for Smart Systems (eds. B. Miara, G. Stavroulakis, V. Valente), World Scientific (2007).

[8] A.M. Katz. Physiology of the Heart. Lippincott Williams & Wilkins, 2006.

[9] D. Burkoff. Mechanical properties of the heart and its interaction with the vascular system. Cardiac Physiology, 1–23, (2002).

[10] K.B. Campbell, A.M. Simpson, S.G. Campbell, H.L. Granzier, B.K. Slinker. Dynamic left ventricular elastance: a model for integrating cardiac muscle contraction into ventricular pressure–volume relationships. J. Appl. Physiol., 104, 958–975, (2008).

[11] J. Merodio, R.W. Ogden. Mechanical response of fiber-reinforced incompressible non-linearly elastic solids, International Journal of Non-Linear Mechanics, **40** (2005).

[12] G.C. Engelmayr Jr., M. Cheng, C.J. Bettinger, J.T. Borenstein, R. Langer, L.E. Freed, 2008. Accordion-like honeycombs for tissue engineering of cardiac anisotropy. Nature Matrials, 8, 1003–1010.

[13] E.K. Rodriguez, W.C. Hunter, M.J. Royce, M.K. Leppo, A.S. Douglas, H.F. Weisman. A method to reconstruct myocardial sarcomere lengths and orientations at transmural sites in beating canine hearts. Am. J. Physiol. Heart Circ. Physiol., 263, H293–H306, 1992.